Travelling wave locomotion of a tensegrity robotic snake based on self-excitation controllers

Xin Li, Jingfeng He, Alexandre Pitti

Travelling wave locomotion of a tensegrity robotic snake based on self-excitation controllers

Xin Li[1,2], Jingfeng He[1], Alexandre Pitti[2]

***Abstract*— The article presents self-excitation methods that aim to achieve the locomotion of a tensegrity robotic snake. The snake-like robot usually forms locomotion by a travelling wave. In this paper, we try to achieve travelling wave locomotion of a tensegrity robotic snake by self-excitation controllers. Two types of self-excitation methods are introduced in this study. These two types of methods are constructed by Kuramoto oscillators and cross-feedback controllers respectively. We derive the total dynamic model of a tensegrity robotic snake and the friction model between wheels and ground. To verify the effectiveness of self-excitation methods, a total dynamic model and two self-excitation controller models are built by numerical software and several simulations are performed. The results of simulations show that travelling wave locomotion can be generated by different self-excitation methods. We also find that controllers, the robotic snake and the environment are coupled to induce limit cycle locomotion of the robot.**

I. INTRODUCTION

A tensegrity structure is composed of compressive and tensile members and their stability is obtained by applying a pre-stress [1]. Tensegrity structures have some advantageous characteristics, such as light weight, high strength-to-weight ratio, high efficiency, and high compliance [2], [3]. Due to these advantageous characteristics, tensegrity structures recently access to the field of robots [4], which have been used in fish robots [2], [5], [6], spherical robots [3], [7]–[9], spine-like robots [10], [11] and etc. In this paper, we model a tensegrity robotic snake by the spine-like structure.

The high compliance of tensegrity robots is prone to induce an oscillatory motion, which is generally avoided in traditional control strategies [12]. However, the characteristic is used by some researchers to explore the locomotion of tensegrity robots. V. Bohm et al. establish a vibration-driven mobile robot based on tensegrity structures. The robot can achieve locomotion using only a single actuator [13]. John Rieffel and Jean-Baptiste Mouret develop a vibration-driven tensegrity mobile robot. They use a machine learning algorithm to discover effective gaits of the robot. The tensegrity robot can move at a fast speed($>$10cm/s) and adapt to new situations with few trials [14]. Bingxing Chen et al. establish a robotic fish with tensegrity joints. The locomotion of the robot is achieved by exciting the dominant vibration mode of the tensegrity structure. The robot can move at a maximum speed of 0.5 body length per cycle [6]. Thomas Bliss et al. develop a robotic swimmer based on a tensegrity structure. A Central Pattern Generator(CPG) controller is designed to achieve entrainment of the tensegrity robot [15]. Brian T. Mirletz et al. develop some tensegrity spines. These robots can traverse irregular terrain controlled by CPG [10]. As mentioned above, it can be seen that vibration-driven tensegrity robots can obtain a good performance of locomotion. In this paper, we construct a vibration-driven tensegrity snake with wheels that is different from robots mentioned above.

In addition, the self-excitation method can usually be used to realize high speed and high efficiency locomotion of robots [16]. Kosuke Tani et al. develop a flapping robot with a self-excitation pneumatic actuator [17]. Alex Pitti explores the natural dynamics of a robot by the self-excitation method [18]. Yuji Miyaki et al. present a self-excited vibration method to induce a travelling wave in a soft mobile robot. The robot can achieve forward locomotion by a travelling wave [19]. Kyosuke Ono et al. propose a self-excitation controller. The self-excitation method is applied to a flutter mechanism [20], a biped robot [21], a robotic fish [22], and a snake robot [16]. Since the self-excitation method utilizes the natural motion of the structure, the method can control the robot to achieve an efficient motion. The biped robot can perform natural dynamic walking on a level floor [21]. For the robotic fish with the self-excitation controller, the maximum speed of locomotion is 0.42m/s [22]. The snake robot can generate a travelling wave by self-excitation control. The maximum locomotion velocity of the snake robot is 0.4m/s [16]. These robots controlled by self-excitation methods obtain good performance in different applications. We want to achieve good locomotion of a tensegrity robotic snake by self-excitation methods in this study. As we know, locomotion of snake robots can be induced by a travelling wave [23], [24]. In this paper, we aim to produce travelling wave locomotion of the tensegrity robotic snake by self-excitation methods.

As we introduced above, robots can achieve good locomotion driven by self-excitation vibration. Thus, we try to control a tensegrity robotic snake to move by self-excitation vibration in this paper. Since the travelling wave is easy to guide locomotion of robotic snake, the focus of this study is to form a travelling wave by self-excitation vibration method.

In this paper, we construct a robotic snake that employs a tensegrity structure, then derive the dynamics of the

*The first author wants to thank China Scholarship Council (CSC, grant number: 202006120172) for the financial support of studying.

[1,2]Xin Li is with School of Mechatronics Engineering, Harbin Institute of Technology, Harbin 150001, China. He studies in ETIS Laboratory, CNRS UMR 8051, CY Cergy-Paris University, as a visiting Ph.D. student between March 2021 and March 2022. xin_li_@outlook.com

[1]Jingfeng He is with School of Mechatronics Engineering, Harbin Institute of Technology, Harbin 150001, China. hjfeng@hit.edu.cn

[2]Alexandre Pitti is with ETIS Laboratory, CNRS UMR 8051, CY Cergy-Paris University, Cergy-Pontoise 95302, France. alexandre.pitti@cyu.fr

tensegrity robotic snake. The robotic snake with wheels will move on the ground. Therefore, it is necessary to derive the friction model between wheels and ground. For the controller of the robot, we introduce two types of self-excitation controllers. These controllers include a CPG network and a self-excitation method with cross-feedback. The CPG network is composed of Kuramoto oscillators with constant phase differences. Finally, we perform the simulations by the numerical simulation software and perform some simulations. The results of simulations show that the travelling wave locomotion of the robot can be achieved by self-excitation controllers. In addition, we can also find that the limit cycle locomotion can be induced by self-excitation method.

In section II, we introduce the structural description and derive the dynamics model and friction model of the tensegrity robotic snake. In section III, we present two types of self-excitation methods. In section IV, simulation models are established by numerical software and some locomotion simulations of a tensegrity robot are performed. Our findings and future work are summarized in section V.

II. ANALYTICAL MODEL OF THE TENSEGRITY ROBOTIC SNAKE

A. Structural Description

In this subsection, we present a structural description of a tensegrity robotic snake. As shown in Fig. 1, a tensegrity robotic snake is composed of 5 rigid bodies and 32 tensile members. In this model, each rigid body is composed of 6 interconnected rods, tensile members includes passive springs and active cables. Excitation signals are applied to the structure by active cables that are placed between the two adjacent segments. Two wheels are placed at the bottom of each rigid body. The length of the robot is 0.34m.

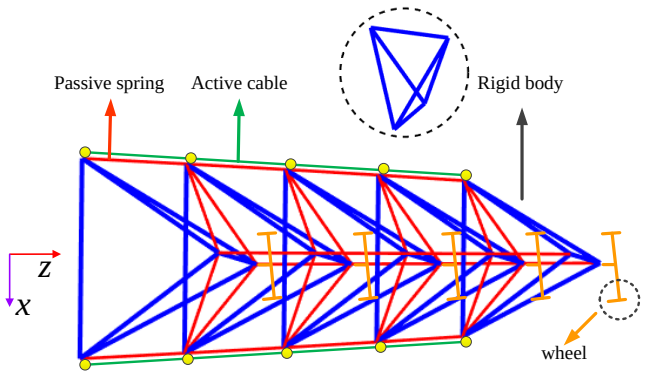

Fig. 1. A tensegrity robotic snake.

A connectivity matrix for a rigid body is represented by $\mathbf{C}$. Suppose member k connects nodes i and j ($i < j$). Then, the ith and jth members of the kth row of $\mathbf{C}$ are set to 1 and -1, respectively [25]. The expression is as follows:

$$\mathbf{C}_{(k,p)} = \begin{cases} 1 & \text{for } p = i \\ -1 & \text{for } p = j \\ 0 & \text{otherwise} \end{cases} \tag{1}$$

The connectivity matrix is a description method of structural topology. It will be used in the derivation of tensegrity robotic dynamics.

B. Dynamics of the Tensegrity Robotic Snake

The dynamic model of the tensegrity robotic snake is derived from the method proposed by R.E. Skelton and K. Nagase [26]. In this model, each rigid body is composed of 6 interconnected rods. Thus, we need to consider geometrical constraints in the dynamic equation as described in the article [26]. The dynamics of the tensegrity snake is represented as follows:

$$\mathbf{M}_c\ddot{\mathbf{n}}_c + \mathbf{K}_c\mathbf{n}_c = \mathbf{B}_c\mathbf{t}_c + \mathbf{H}\bar{\mathbf{C}}_B\mathbf{f}_{nc} - \mathbf{N}_d \tag{2}$$

where $\mathbf{n}_c$ is the coordinate vector of free nodes, $\mathbf{t}_c$ is the magnitude vector of the constraint forces, and $\mathbf{f}_{nc}$ is the vector of the nodal forces. $\mathbf{M}_c$, $\mathbf{K}_c$, $\mathbf{B}_c$, $\mathbf{N}_d$, $\mathbf{H}\bar{\mathbf{C}}_B$ are terms of total dynamics equation. The detailed derivations of these terms are presented in the paper [26].

The nodal forces of the tensegrity robotic snake is presented as follows:

$$\mathbf{f}_{n_c} = \mathbf{w} + \mathbf{f}_s + \mathbf{f}_g \tag{3}$$

where $\mathbf{w}$ is the sum of the external forces, which includes friction forces and forces of the active cables. $\mathbf{f}_s$ is the force vector of passive springs, and $\mathbf{f}_g$ is the gravity force vector.

C. Friction Model

The tensegrity robotic snake moves in the x-z plane. Thus, we derive the friction model in the x-z plane. For the convenience of representation, we draw a simplified diagram in Fig. 2. The model of asymmetric friction between the wheels and ground is derived from the method presented in the paper [16].

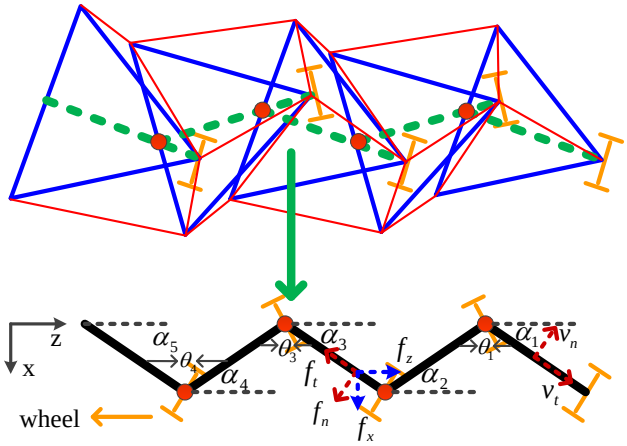

Fig. 2. A simplified diagram of the tensegrity robotic snake.

The relation between the velocity of tangential and normal direction and that of x and z direction is derived as follows:

$$\begin{bmatrix} v_{ti} \\ v_{ni} \end{bmatrix} = \begin{bmatrix} s_i & c_i \\ -c_i & s_i \end{bmatrix} \begin{bmatrix} v_{xi} \\ v_{zi} \end{bmatrix} \tag{4}$$

where $s_i = \sin\alpha_i$, $c_i = \cos\alpha_i$. v_{ti} and v_{ni} are velocities of the tangential and normal direction. v_{xi} and v_{zi} are velocities of the x and z direction.

Tangential and normal friction forces are represented as follows:

$$\mathbf{f}_{ti} = -\mu_t m_i g(\mathrm{sig}(v_{ti})) \tag{5}$$

$$\mathbf{f}_{ni} = \begin{cases} -\frac{1}{\gamma}\mu_n m_i g \left|\frac{v_{ni}}{v_{ti}}\right| (\mathrm{sig}(v_{ni})) & (\frac{v_{ni}}{v_{ti}} \le \gamma) \\ -\mu_n m_i g(\mathrm{sig}(v_{ni})) & (\frac{v_{ni}}{v_{ti}} > \gamma) \end{cases} \tag{6}$$

where μ_t and μ_n are tangential and normal friction coefficients. γ is the traction parameter. m_i is the mass of the ith segment of the tensegrity snake. g is coefficient of gravity.

The friction forces between the wheels and ground are derived as follows:

$$\begin{bmatrix} f_{xi} \\ f_{zi} \end{bmatrix} = \begin{bmatrix} -s_i & c_i \\ -c_i & -s_i \end{bmatrix} \begin{bmatrix} f_{ti} \\ f_{ni} \end{bmatrix} \tag{7}$$

Then, we can obtain total friction force between the robotic snake and ground by the method. The friction force is integrated into the dynamic model Eq.(2) as the external force, then we can obtain the total dynamic of tensegrity robotic snake.

III. SELF-EXCITATION METHOD

A. Self-excitation Method with Kuramoto Oscillators

In this subsection, we construct a self-excitation system by a CPG network. The network is composed of Kuramoto oscillators with constant phase differences. An error-driven Proportional-Derivative (PD) controller is used to control active cables.

As shown in Fig. 1, we take 4 pairs of active cables to excite the tensegrity snake and construct a CPG network with 4 pairs of Kuramoto oscillators. The phase difference of each pair of oscillators is π. Each pair of oscillators excite two antagonistic cables respectively. The network is shown in the Fig. 3.

The Kuramoto oscillator model is denoted as follow:

$$\frac{dv_i}{dt} = \omega_i + \mathrm{KE}\sin(\theta_i - v_i) + \frac{\mathrm{KI}}{N}\sum_{j=1}^{N}(v_j - v_i - \varphi_{ij}) \tag{8}$$

$$u_i = \mathrm{JE}\sin(v_i) \tag{9}$$

$$\mathrm{JE} = \mathrm{K}_p(\theta_i - v_i) + \mathrm{K}_d(\dot{\theta}_i - \dot{v}_i) \tag{10}$$

where KE and KI are external and internal coupling coefficients of oscillators respectively. v_i and v_j are the output signals of the ith and jth oscillators. φ_{ij} is the phase difference between the ith and jth oscillators. θ_i is the ith angle of the tensegrity robotic snake. JE is a Proportional-Derivative controller to control the angles in the high level. K_p and K_d are the proportional and derivative gains of the PD controller.

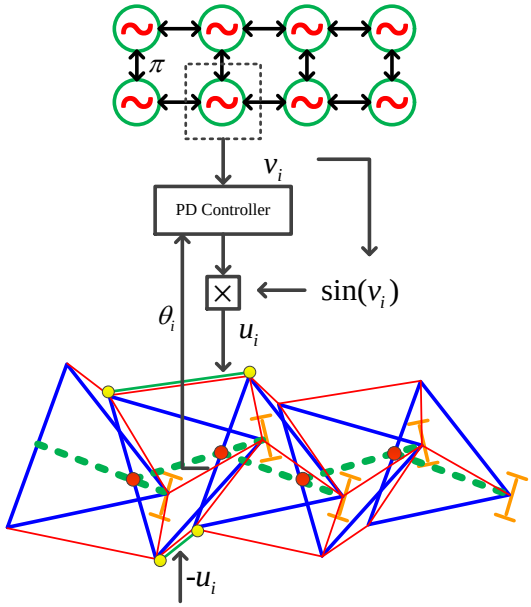

Fig. 3. CPG network used in the tensegrity robotic snake.

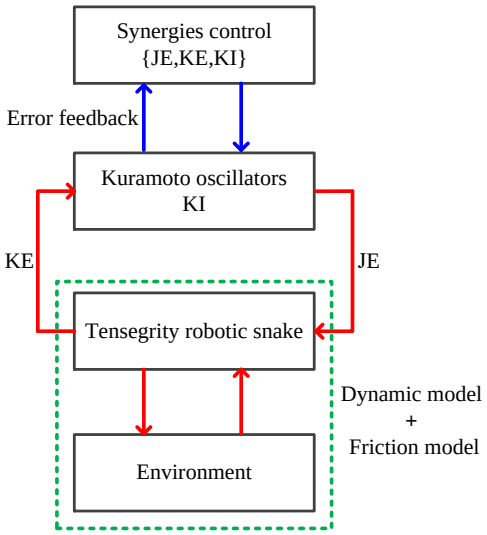

Fig. 4. General model for control of the tensegrity robotic snake.

The internal coupling coefficient KI makes different oscillators form a phase difference. Due to the phase difference of the oscillators, the travelling wave locomotion of a tensegrity robotic snake can be formed. The external coupling coefficient KE makes oscillators couple with the robotic dynamics. Since the friction model is also included in the dynamics model. Oscillators, a tensegrity robotic snake, and environment are coupled during the locomotion of the robot. Thus, we can obtain the general model for control of the tensegrity robotic snake as shown in Fig. 4.

B. Self-excitation Method with Cross-feedback

In this subsection, we construct a self-excitation controller of the tensegrity robotic snake by cross-feedback. The self-excitation method has been used for robotic snakes and fish

[16], [22]. In this paper, the travelling wave locomotion of a tensegrity robotic snake can be formed by the self-excitation controller. In this controller, the self-excitation oscillation can be generated by the cross-feedback. As shown in Fig. 5, the ith angle between the ith and i+1th segments is used as the feedback signal of the i+1th active cable controller.

The input signal of the i+1th active cable controller is expressed as follows:

$$T_{i+1} = \alpha\theta_i \tag{11}$$

where α is the feedback gain, θ_i is the ith feedback angle, T_{i+1} is the output signal of the i+1th active cable controller. In this system, we need to control a pair of active cables between neighboring segments, the output signal of one cable controller is T_{i+1} and another one is $-T_{i+1}$.

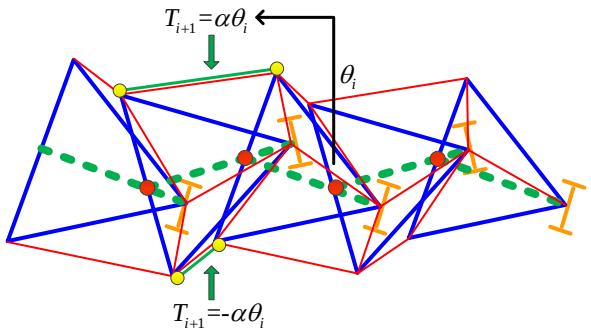

Fig. 5. The self-oscillation controller by cross-feedback.

In this system, the cross-feedback term creates an asymmetric stiffness matrix of the tensegrity robotic snake, which has a possibility to form a self-excitation oscillation system [16], [22].

IV. NUMERICAL SIMULATION

A. Travelling Wave Locomotion by CPG

In this subsection, a total dynamic model and a CPG network with 8 oscillators are established by the numerical simulation software. In this simulation, the phase difference between adjacent oscillators on the same side is set to $\pi/2$. To obtain better performances, we search for the appropriate parameters of a controller by multiple simulations. These parameters include frequency, coupling coefficients and gains of PD controllers. We find that the tensegrity robotic snake has a better performance when the frequency of oscillators is around 5Hz.

The output amplitude of a controller is limited by an ideal relay function. Distances of different simulations are shown in the Fig. 6. It is evident that the larger output amplitude of the controller will induce a faster locomotion of the tensegrity robotic snake.

From the Fig. 7, it's readily apparent that the CPG network produces a travelling wave, which is caused by internal coupling of oscillators and the constant phase difference between neighbouring oscillators.

As shown in the Fig. 7, there is no phase difference at the beginning of the simulation. Due to the effect of

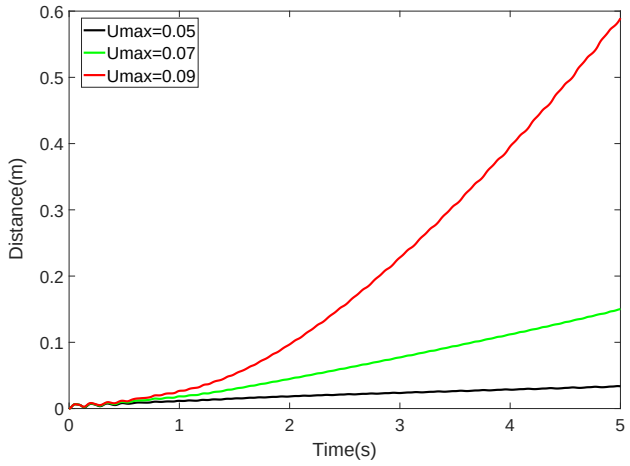

Fig. 6. Distance curves of the robot by CPG controller.

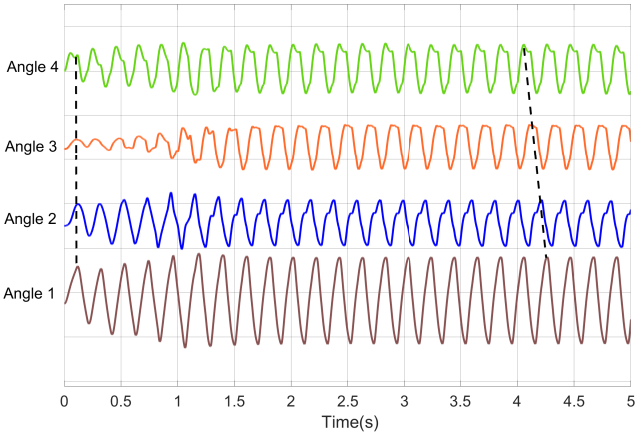

Fig. 7. Travelling wave formed by CPG controller.

the internal coupling coefficient, oscillators of the network gradually produce a phase difference. Thus, a travelling wave locomotion of the tensegrity robotic snake is formed.

It is evident from Fig. 8 that a limit cycle is formed in this simulation. It shows that the robotic snake, oscillators and environment are coupled to induce a limit cycle oscillation by the coupling coefficients.

In the next subsection, we will introduce a relatively simple self-excitation method to form travelling wave locomotion of the tensegrity robotic snake.

B. Travelling Wave Locomotion by Cross-feedback

In this subsection, a total dynamics model and a cross-feedback controller are built by the numerical simulation software. We perform some simulations in this subsection. In these simulations, output amplitudes of controllers are limited by ideal relay functions. We set different limit amplitudes of ideal relay functions and obtain robotic distances of different simulations. The relationship between the output amplitude of the controller and the velocity of robotic locomotion is explored by comparing these data.

We can obtain different distance curves of the robot when the output amplitude of the controller changes from 0.05 to

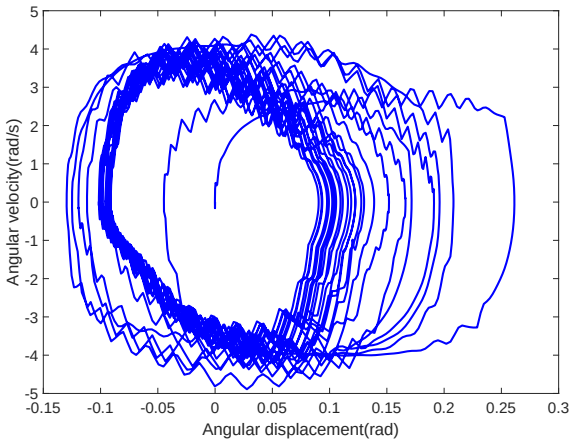

Fig. 8. Limit cycle locomotion by CPG controller.

0.2. The different distance curves of robots are shown in the Fig. 9. From the figure, we can find that the velocity of robotic locomotion increases with the output amplitude of the controller. The larger output amplitude of the controller will cause the robot to produce a larger swing amplitude. The robotic velocity will increase with the swing amplitude of the robot. This conclusion is consistent with the research conclusions in the paper [28].

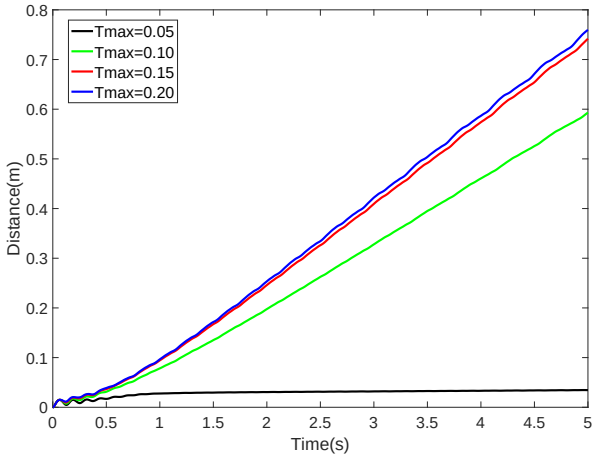

Fig. 9. Distance curves of the robot by cross-feedback controller.

The locomotion of the tensegrity robotic snake is shown in Fig. 10. It is evident from the figure that the tensegrity robotic snake moves along the z direction.

The locomotion of the tensegrity robotic snake is induced by the self-excitation controller. Due to the stiffness matrix becomes an asymmetrical matrix by the active cable input, the controller has a possibility to induce a self-excitation oscillation [16]. A travelling wave is produced by the self-excitation controller with cross-feedback signals. The travelling wave is shown in the Fig. 11. It is evident that a travelling wave is formed at the beginning of the simulation. Thus, the controller is easier than the CPG controller to maintain the forward direction of the tensegrity robotic

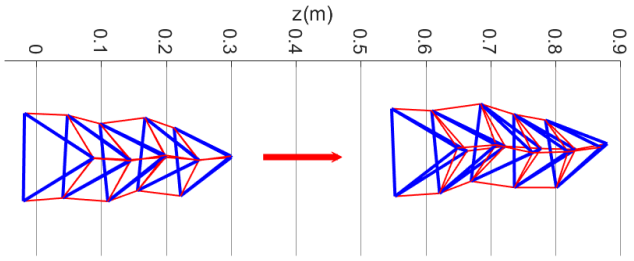

Fig. 10. Locomotion of the robot by cross-feedback controller.

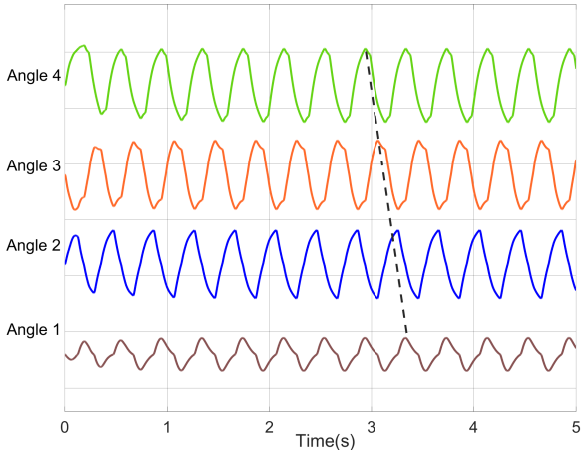

Fig. 11. Travelling wave formed by the cross-feedback controller.

snake. However, if the robot moves at a faster speed, we still need a direction controller. In addition, there are a few parameters for the self-excitation controller with cross-feedback.

In this simulation, a limit cycle locomotion is also induced by the self-excitation controller. As shown in Fig. 12, the tensegrity robotic snake excited by a self-excitation controller couple with the environment to form limit cycle locomotion.

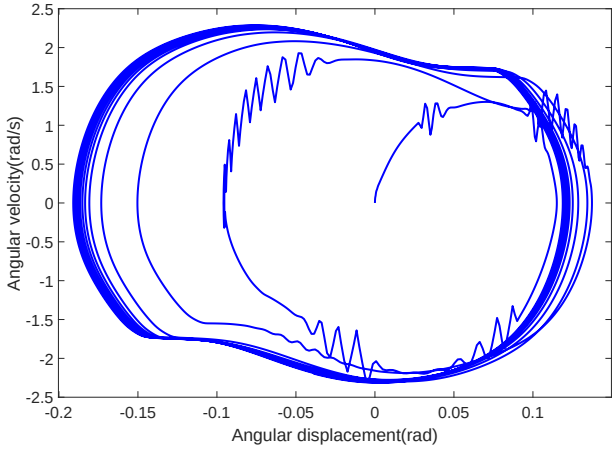

Fig. 12. Limit cycle locomotion by the cross-feedback controller.

V. CONCLUSION AND FUTURE WORK

In this paper, a total dynamics model composed of dynamics of tensegrity robotic snake and friction model between

wheels and ground is derived. Two types of self-excitation methods are presented in this paper. Simulations of robotic locomotion are performed by numerical software. We perform simulations and find that the travelling wave locomotion of the tensegrity robotic snake can be formed by these two types of self-excitation methods. In addition, the robot, controllers and environment are coupled to form a limit cycle oscillation during robotic locomotion. By comparing the two self-excitation methods, we find that the self-excitation method with cross-feedback is easier to form a travelling wave. A few parameters that need to be controlled for the self-excitation method with cross-feedback. The research provides a theoretical basis for the experiment of robotic locomotion. In the future, we will establish a prototype of the tensegrity robotic snake and perform locomotion tests on the ground.

ACKNOWLEDGMENT

The first author wants to thank China Scholarship Council (CSC, grant number: 202006120172) for the financial support of studying.

REFERENCES

[1] R. E. Skelton and M. C. De Oliveira, *Tensegrity systems*. New York: Springer, 2009.

[2] B. Chen and H. Jiang, "Body stiffness variation of a tensegrity robotic fish using antagonistic stiffness in a kinematically singular configuration," *IEEE Transactions on Robotics*, pp. 1–16, 2021.

[3] J. Luo, R. Edmunds, F. Rice, and A. M. Agogino, "Tensegrity robot locomotion under limited sensory inputs via deep reinforcement learning," in *2018 IEEE International Conference on Robotics and Automation (ICRA)*. IEEE, 2018, pp. 6260–6267.

[4] P. Schorr, L. Zentner, K. Zimmermann, and V. Böhm, "Jumping locomotion system based on a multistable tensegrity structure," *Mechanical Systems and Signal Processing*, vol. 152, p. 107384, 2021.

[5] J. Shintake, D. Zappetti, T. Peter, Y. Ikemoto, and D. Floreano, "Bio-inspired tensegrity fish robot," in *2020 IEEE International Conference on Robotics and Automation (ICRA)*. IEEE, 2020, pp. 2887–2892.

[6] B. Chen and H. Jiang, "Swimming performance of a tensegrity robotic fish," *Soft robotics*, vol. 6, no. 4, pp. 520–531, 2019.

[7] M. Zhang, X. Geng, J. Bruce, K. Caluwaerts, M. Vespignani, V. SunSpiral, P. Abbeel, and S. Levine, "Deep reinforcement learning for tensegrity robot locomotion," in *2017 IEEE International Conference on Robotics and Automation (ICRA)*. IEEE, 2017, pp. 634–641.

[8] M. Vespignani, J. M. Friesen, V. SunSpiral, and J. Bruce, "Design of superball v2, a compliant tensegrity robot for absorbing large impacts," in *2018 IEEE/RSJ International Conference on Intelligent Robots and Systems (IROS)*. IEEE, 2018, pp. 2865–2871.

[9] A. P. Sabelhaus, J. Bruce, K. Caluwaerts, P. Manovi, R. F. Firoozi, S. Dobi, A. M. Agogino, and V. SunSpiral, "System design and locomotion of superball, an untethered tensegrity robot," in *2015 IEEE international conference on robotics and automation (ICRA)*. IEEE, 2015, pp. 2867–2873.

[10] B. T. Mirletz, P. Bhandal, R. D. Adams, A. K. Agogino, R. D. Quinn, and V. SunSpiral, "Goal-directed cpg-based control for tensegrity spines with many degrees of freedom traversing irregular terrain," *Soft Robotics*, vol. 2, no. 4, pp. 165–176, 2015.

[11] A. Melnyk and A. Pitti, "Synergistic control of a multi-segments vertebral column robot based on tensegrity for postural balance," *Advanced Robotics*, vol. 32, no. 15, pp. 850–864, 2018.

[12] X. Li, J. He, M. Li, H. Jiang, and Y. Huang, "Modal analysis method for tensegrity structures via stiffness transformation from node space to task space," *Engineering Structures*, vol. 203, p. 109881, 2020.

[13] V. Böhm and K. Zimmermann, "Vibration-driven mobile robots based on single actuated tensegrity structures," in *2013 IEEE international conference on robotics and automation*. IEEE, 2013, pp. 5475–5480.

[14] J. Rieffel and J.-B. Mouret, "Adaptive and resilient soft tensegrity robots," *Soft robotics*, vol. 5, no. 3, pp. 318–329, 2018.

[15] T. Bliss, T. Iwasaki, and H. Bart-Smith, "Central pattern generator control of a tensegrity swimmer," *IEEE/ASME Transactions on Mechatronics*, vol. 18, no. 2, pp. 586–597, 2012.

[16] J. Ute and K. Ono, "Fast and efficient locomotion of a snake robot based on self-excitation principle," in *7th International Workshop on Advanced Motion Control. Proceedings (Cat. No. 02TH8623)*. IEEE, 2002, pp. 532–539.

[17] K. Tani, H. Nabae, G. Endo, and K. Suzumori, "Proposal and prototyping of self-excited pneumatic actuator using automatic-flow-path-switching-mechanism," *IEEE Robotics and Automation Letters*, vol. 5, no. 2, pp. 3058–3065, 2020.

[18] A. Pitti, M. Lungarella, and Y. Kuniyoshi, "Exploration of natural dynamics through resonance and chaos," in *Proc. 9th Conf. on Intelligent Autonomous Systems*, Tokyo, Japan, 2006, pp. 558–565.

[19] Y. Miyaki and H. Tsukagoshi, "Self-excited vibration valve that induces traveling waves in pneumatic soft mobile robots," *IEEE Robotics and Automation Letters*, vol. 5, no. 3, pp. 4133–4139, 2020.

[20] K. Ono and T. Okada, "Self-excited vibratory system for a flutter mechanism (special issue on nonlinear dynamics)," *JSME International Journal Series C Mechanical Systems, Machine Elements and Manufacturing*, vol. 41, no. 3, pp. 621–629, 1998.

[21] K. Ono, T. Furuichi, and R. Takahashi, "Self-excited walking of a biped mechanism with feet," *The International Journal of Robotics Research*, vol. 23, no. 1, pp. 55–68, 2004.

[22] M. Nakashima, N. Ohgishi, and K. Ono, "A study on the propulsive mechanism of a double jointed fish robot utilizing self-excitation control," *JSME International Journal Series C Mechanical Systems, Machine Elements and Manufacturing*, vol. 46, no. 3, pp. 982–990, 2003.

[23] A. Crespi and A. J. Ijspeert, "Online optimization of swimming and crawling in an amphibious snake robot," *IEEE Transactions on Robotics*, vol. 24, no. 1, pp. 75–87, 2008.

[24] A. J. Ijspeert and A. Crespi, "Online trajectory generation in an amphibious snake robot using a lamprey-like central pattern generator model," in *Proceedings 2007 IEEE International Conference on Robotics and Automation*. IEEE, 2007, pp. 262–268.

[25] J. Zhang and M. Ohsaki, "Adaptive force density method for form-finding problem of tensegrity structures," *International Journal of Solids and Structures*, vol. 43, no. 18-19, pp. 5658–5673, 2006.

[26] K. Nagase and R. Skelton, "Network and vector forms of tensegrity system dynamics," *Mechanics Research Communications*, vol. 59, pp. 14–25, 2014.

[27] X. Liu, R. Gasoto, Z. Jiang, C. Onal, and J. Fu, "Learning to locomote with artificial neural-network and cpg-based control in a soft snake robot," in *2020 IEEE/RSJ International Conference on Intelligent Robots and Systems (IROS)*. IEEE, 2020, pp. 7758–7765.

[28] A. Crespi, A. Badertscher, A. Guignard, and A. J. Ijspeert, "Amphibot i: an amphibious snake-like robot," *Robotics and Autonomous Systems*, vol. 50, no. 4, pp. 163–175, 2005.